An analysis of the initial-value wavemaker problem

By S. W. JOO[1], W. W. SCHULTZ[1] AND A. F. MESSITER[2]

[1] Department of Mechanical Engineering and Applied Mechanics, University of Michigan, Ann Arbor, MI 48109, USA

[2] Department of Aerospace Engineering, University of Michigan, Ann Arbor, MI 48109, USA

A Fourier-integral method is developed to obtain transient solutions to potential wavemaker problems. This method yields solutions for wavemaker velocities which need not be given as powers of time. The results are compared with known small-time and local solutions. Examples considered include ramp, step, and harmonic wavemaker velocities. As time becomes large, the behaviour near the wave front is derived for the impulsive wavemaker, and for the harmonic wavemaker it is shown that the steady-state solution is recovered. The solution for a wavemaker velocity given as a Fourier cosine series compares favourably with available experimental results. Capillary effects are included and nonlinear effects are discussed.

1. Introduction

The study of water waves associated with surface-piercing bodies has long been an interesting and important area in fluid mechanics. In many cases, however, both analysis and computation run into difficulties near the intersection of a body with the free surface. To examine this problem, a number of researchers have used a small-time expansion to consider a vertical wavemaker moving horizontally in a fluid of finite depth. Peregrine (1972) used a moving coordinate system attached to the wavemaker, noted a logarithmic singularity at the contact line, and explained the necessity of a local solution. Chwang (1983) obtained a solution with a stationary coordinate system and argued that the singularity lies outside of the physical domain. Therefore, he did not proceed further to obtain the local solution required near the contact line. The singular behaviour in the small-time solution was confirmed by Lin (1984) by a Lagrangian description of the problem.

In an earlier work, Kennard (1949) developed an integral representation of the linear solution by use of distributed sources along the wavemaker and gave an application to an oscillating wavemaker. Madsen (1970) compared this representation with experimental data and added a discussion of second-order terms. It was not until the work of Roberts (1987) that a successful local analysis for the power-law movement of the wavemaker was carried out for small time and small Froude number. Using a Laplace transformation and expanding the result for small time, he found that the solution varies significantly in the neighbourhood of the contact line and gave a self-similar formulation to describe this behaviour. If the wavemaker starts to move impulsively (step velocity), however, the neglected nonlinear effect becomes important close to the wavemaker, since the linearized vertical velocity becomes infinitely large as time becomes smaller.

As noted by Roberts (1987), a proper treatment of the singularity at the contact line cannot be achieved by a small-time expansion derived for infinitesimal time with

the distance from the wavemaker fixed. A correct local solution requires a new lengthscale that varies in time. In other words, very near the contact line spatial variables are coupled with time, so that the small-time expansion does not yield a well-behaved solution there. The present study uses a small-amplitude expansion and a Fourier integral representation, for arbitrary time and distance. It is also possible to include the effects of surface tension and prescribed contact angle with little added effort in the integral representation. A number of examples are considered, and various limits of the solution are studied. For viscous fluids the unsteady motion of the contact line, with the no-slip condition incorporated at the body, would require special consideration, as discussed in the review by Dussan V. (1979) and in an application to water waves by Hocking (1987). We shall not consider such complications here.

We begin in §2 by introducing the formulation of the vertical wavemaker problem. The velocity of the wavemaker is given as a function of time, and the surface tension on the free surface is retained with non-zero static contact angle. In §§3 and 4 we consider two hypothetical wavemaker velocities, expressed by ramp and step functions in time. The solutions for zero surface tension are shown to agree with the local solutions of Roberts (1987) for small time near the contact line; the self-similar form is noted. Also, sufficiently far from the contact line, they are shown to agree with the small-time solution of Peregrine (1972). These results were shown explicitly by Roberts (1987) and could also have been found by evaluation of integrals given by Kennard (1949). The nonlinear formulation and large-time behaviour for the step velocity are also discussed.

More general types of wavemaker velocities are discussed in §§5 and 6. One example is a more realistic velocity that starts from zero and increases toward a finite constant value. It is shown how the solutions for step and ramp velocities can be recovered as limiting cases. In §6, the present method allows a transient solution for a simple-harmonic wavemaker. Sufficiently far from the contact line and in the limit as time approaches infinity, the solution agrees with that of Havelock (1929), as cited by Yih (1979). As a final example in §6, we examine a wavemaker velocity considered by Dommermuth et al. (1988) and compare our analytical solution with their experimental results.

This study is prompted, in part, by computational difficulties caused by bodies intersecting free surfaces. These include high-wavenumber oscillations close to the contact line that may imply a physical or numerical instability. Normally, the spatial dependence is solved by a boundary-integral approach, but these techniques are known to have difficulties with corners, even when singular behaviour is not present (Schultz & Hong 1989). The standard approach is to separate the spatial and temporal behaviour, thus introducing the logarithmic singularity into the problem as mentioned above. However, this singular behaviour is not modelled correctly by standard (piecewise-polynomial) boundary-integral algorithms, and is further complicated by the errors associated with corners. Therefore, it is fortuitous that accurate computational results are obtained for regions not too close to the wavemaker (Dommermuth et al. 1988). A special fully implicit time-marching scheme should be developed for precise computations near the contact line.

2. Formulation

We consider the fluid motion due to a moving wall as shown in figure 1. If the fluid is inviscid and incompressible, and the motion starts from rest, the flow will be
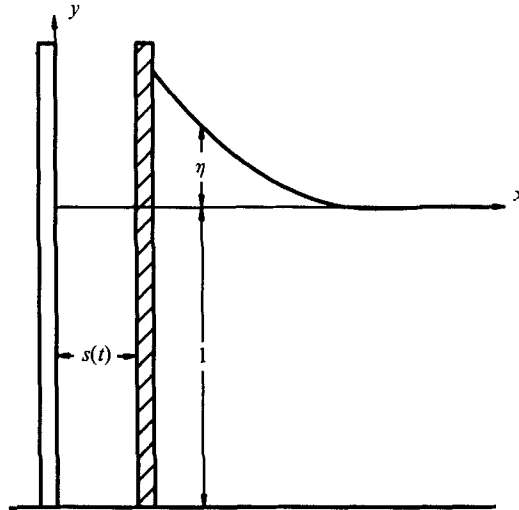
FIGURE 1. Wavemaker configuration.

irrotational according to Kelvin's theorem and is described by the Laplace equation. In non-dimensional variables

$$\phi_{xx} + \phi_{yy} = 0 \quad \text{for} \quad x > s(t), \quad -1 < y < \eta(x,t), \tag{1}$$

where $\phi(x,y,t)$ is the velocity potential, $\eta(x,t)$ is the free-surface elevation measured from the undisturbed level at infinity, and $s(t)$ is the displacement of the wall from its initial location, which, of course, is the time integral of the wavemaker velocity. The velocity, length, and time scales are chosen to be $(gh)^{\frac{1}{2}}, h, (h/g)^{\frac{1}{2}}$, where h is the undisturbed depth of the fluid and g is the gravitational acceleration. The fluid velocity at the wavemaker is prescribed as

$$\phi_x = \alpha u(t) \quad \text{on} \quad x = s(t), \tag{2}$$

where α is the Froude number. For example, if the dimensional wavemaker velocity, U, is given as a function of non-dimensional time by

$$U = C\left[\left(\frac{h}{g}\right)^{\frac{1}{2}} t\right]^q, \quad t > 0, \tag{3}$$

where C and q are constants, we have

$$\alpha = \frac{C}{(g^{1+q} h^{1-q})^{\frac{1}{2}}}.$$

Thus, $u(t)$ and $s(t)$ in (2) become

$$u(t) = t^q, \quad s(t) = \alpha t^{q+1}/(q+1).$$

In particular, the cases for $q = 0$ and $q = 1$ correspond to a step velocity and a ramp velocity, respectively.

This $u(t)$ describes a power-law movement of the wavemaker, which can approximate the earlier stages of a more general motion for small time and, thus, is frequently used in small-time analyses. In the present work, however, the general expression for $u(t)$ will be maintained and a solution valid for all time will be sought.

In the presence of non-zero surface tension, the kinematic and dynamic boundary conditions on the free surface become

$$\phi_y = \eta_t + \phi_x \eta_x \quad \text{on} \quad y = \eta, \tag{4}$$

$$\phi_t + \tfrac{1}{2}(\phi_x^2 + \phi_y^2) + \eta - \frac{T\eta_{xx}}{(1+\eta_x^2)^{\frac{3}{2}}} = 0 \quad \text{on} \quad y = \eta, \tag{5}$$

where the non-dimensional surface tension T, the reciprocal of the Bond number, is defined by

$$T = \frac{\sigma}{\rho g h^2}.$$

Here, σ is the surface-tension constant, and ρ is the density of the fluid. On the bottom, the vertical velocity component vanishes, so that

$$\phi_y = 0 \quad \text{on} \quad y = -1. \tag{6}$$

Since the motion starts from rest, the initial conditions are

$$\phi = 0, \quad t < 0, \tag{7}$$

$$\eta = \alpha \kappa_0 T^{\frac{1}{2}} \exp\left(-\frac{x}{T^{\frac{1}{2}}}\right), \quad t < 0. \tag{8}$$

Here, κ_0 is a constant determined by $\kappa_0 = \alpha^{-1} \tan\left(\tfrac{1}{2}\pi - \theta_s\right)$ and taken to be $O(1)$, where θ_s is the static contact angle. The initial free-surface elevation (8) satisfies the static linear equivalent of (5) for small κ_0 and becomes zero in the limit as the surface tension becomes zero or the initial contact angle becomes 90°.

Instead of introducing a small-time expansion, which is not valid near the contact line, we now use an expansion for small Froude number. The velocity potential and the free-surface elevation are expanded as

$$\phi(x, y, t) = \alpha\phi_1(x, y, t) + \alpha^2\phi_2(x, y, t) + \dots, \tag{9}$$

$$\eta(x, t) = \alpha\kappa(t) T^{\frac{1}{2}} \exp\left(-\frac{x}{T^{\frac{1}{2}}}\right) + \alpha\eta_1(x, t) + \alpha^2\eta_2(x, t) + \dots, \tag{10}$$

where κ is prescribed using the dynamic contact angle, with $\kappa(0) = \kappa_0$ from (8). Although T is typically very small, we retain $T = O(1)$ in the Fourier integral representations derived below.

Expanding the free-surface boundary conditions and the boundary condition on the wavemaker about $y = 0$ and $x = 0$, respectively, gives the equations to leading order, $O(\alpha)$, as

$$\phi_{1xx} + \phi_{1yy} = 0 \quad \text{for} \quad x > 0, \quad -1 < y < 0, \tag{11}$$

$$\phi_{1x} = u(t) \quad \text{on} \quad x = 0, \tag{12}$$

$$\phi_{1y} = \kappa' T^{\frac{1}{2}} \exp\left(-\frac{x}{T^{\frac{1}{2}}}\right) + \eta_{1t} \quad \text{on} \quad y = 0, \tag{13}$$

$$\phi_{1t} + \eta_1 - T\eta_{1xx} = 0 \quad \text{on} \quad y = 0, \tag{14}$$

$$\phi_{1y} = 0 \quad \text{on} \quad y = -1, \tag{15}$$

where the prime denotes differentiation with respect to time. The boundary condition (12) requires the distance $s(t)$ to be small, so that a restriction should be imposed on

t, depending on the velocity $u(t)$. For the step velocity, for example, the condition is $t \ll (1/\alpha)$. This constraint could be relaxed by applying a simple coordinate transformation $x' = x - s(t)$ to fix the location of the wavemaker at $x' = 0$, which leaves the first-order equations (11)–(15) unchanged. However, for large time it should be expected that the cumulative effect of omitted nonlinear terms will no longer be negligible, and that η_2 and ϕ_2 will become large. For example, since the non-dimensional wave speed in shallow water is $dx/dt = 1 + O(\alpha)$, we may anticipate that the expansions (9) and (10) are valid for large t only if αt is small. We have chosen to retain a fixed coordinate system, since the solutions are asymptotically correct as $\alpha \to 0$ and $\alpha t \to 0$ and since the exact equations, needed again later, are slightly simpler in form. In the figures below, however, it is appropriate to regard x as measured from the wavemaker surface if the solution is to be used at some non-vanishing small value of α.

In solving (11)–(15), we first decompose ϕ_1 into two parts:

$$\phi_1 = 2u(t) \sum_{n=0}^{\infty} \frac{1}{k_n^2} e^{-k_n x} \sin k_n y + \phi_1^*(x, y, t), \tag{16}$$

where $k_n = (n + \frac{1}{2})\pi$. The series on the right-hand side satisfies the Laplace equation and all the boundary conditions except on the free surface, where it becomes zero. The remaining term ϕ_1^*, then, can be considered as a correction that enables the complete solution to satisfy appropriate free-surface boundary conditions. Substitution of (16) into (11)–(15) yields

$$\phi_{1xx}^* + \phi_{1yy}^* = 0 \quad \text{for} \quad x > 0, \quad -1 < y < 0, \tag{17}$$

$$\phi_{1x}^* = 0 \quad \text{on} \quad x = 0, \tag{18}$$

$$-\frac{2}{\pi} u(t) \ln (\tanh \tfrac{1}{4}\pi x) + \phi_{1y}^* = \kappa' T^{\frac{1}{2}} \exp\left(-\frac{x}{T^{\frac{1}{2}}}\right) + \eta_{1t} \quad \text{on} \quad y = 0, \tag{19}$$

$$\phi_{1t}^* + \eta_1 - T\eta_{1xx} = 0 \quad \text{on} \quad y = 0, \tag{20}$$

$$\phi_{1y}^* = 0 \quad \text{on} \quad y = -1. \tag{21}$$

The solution for ϕ_1^* is sought as a Fourier cosine integral:

$$\phi_1^* = \int_0^{\infty} A(k, t) \cosh [k(y+1)] \cos kx \, dk, \tag{22}$$

which already satisfies (17), (18), and (21). The solution for η_1 is then also a Fourier cosine integral:

$$\eta_1 = \int_0^{\infty} B(k, t) \cos kx \, dk. \tag{23}$$

Substituting the representations (22) and (23) into the free-surface conditions (19) and (20) and eliminating B gives

$$A_{tt} \cosh k + k(1 + Tk^2) A \sinh k = -\frac{2u(t)}{\pi}\left(\frac{1}{k} + Tk\right) \tanh k + \frac{2}{\pi}\kappa' T \tag{24}$$

by making use of

$$\int_0^{\infty} \tanh k \cos kx \, \frac{dk}{k} = -\ln (\tanh \tfrac{1}{4}\pi x) \tag{25}$$

(Gradshteyn & Ryzhik 1980). Equation (24) has a general solution

$$A = A_p(k, t) + c_1(k) \sin \beta t + c_2(k) \cos \beta t, \tag{26}$$

where
$$\beta = [k(1 + Tk^2) \tanh k]^{\frac{1}{2}}.$$

Here, A_p is a particular solution of (24) for given $u(t)$ and $\kappa(t)$, and c_1 and c_2 are to be determined from the initial conditions. In most of the following, we shall consider a time-invariant contact angle and set $\kappa = 0$. The extension for time-dependent contact angle can easily be done by retaining the term proportional to κ' in (24).

The Laplace equation does not require any initial condition. Since the time derivatives appear only in the free-surface boundary conditions, the initial conditions are applied on the free surface. The initial condition for η, (8), is converted into a condition for ϕ through (5). Using (9) and (10) again, we then obtain

$$\phi_1 = 0 \quad \text{and} \quad \phi_{1t} = 0$$

at $y = 0$ and $t = 0$. Since the series in (16) is always zero at $y = 0$, through (22)

$$A(k, 0) = A_t(k, 0) = 0. \tag{27}$$

The solution (26), then, is completely determined, and so is ϕ_1^*.

Once ϕ_1^* is obtained, the first-order free-surface elevation, η_1, is given either by (19) or by (20). The vertical velocity,

$$\phi_{1y} = -\frac{2}{\pi} u(t) \ln (\tanh \tfrac{1}{4}\pi x) + \int_0^\infty kA(k, t) \sinh k \cos kx \, dk,$$

has a logarithmic singularity in the first term, which is cancelled by the same singularity in the second term. This will be examined in greater detail for each specific case in the following sections.

The higher-order velocity potentials also satisfy the Laplace equation with a Neumann condition on the wavemaker, so that the same Fourier-integral method as for ϕ_1 can be used. However, in most cases we do not evaluate the Fourier integral for ϕ_1 or η_1 to obtain exact closed-form solutions. Thus, the non-homogeneous terms in the higher-order analysis contain some products of Fourier integrals, which makes numerical analysis inevitable except for certain cases.

3. Ramp velocity

The power-law behaviour of the wavemaker, as given by (3), deserves special attention, because it can expose the initial evolution of the fluid motion without unnecessary complication. Owing to the obvious distinction between the ramp and step velocities, separate consideration will be given to each case.

The ramp velocity represents a wavemaker that starts from rest and increases in speed linearly with time. It corresponds to the case when $q = 1$ in (3), so that the Froude number, α, and the dimensionless velocity, $u(t)$, in (2) become

$$\alpha = \frac{C}{g} \quad \text{and} \quad u(t) = t. \tag{28}$$

Therefore, the expansions in (9) and (10) require small acceleration of the wavemaker.

Application of the Fourier-integral method explained in the previous section yields (24) with $u(t) = t$. The solution satisfying (27) is

$$A(k,t) = -\frac{2}{\pi}\frac{1}{k^2 \cosh k}\left(t - \frac{\sin\beta t}{\beta}\right). \tag{29}$$

Then, from (22) and (16), the first-order velocity potential is obtained as

$$\phi_1 = 2t\sum_{n=0}^{\infty}\frac{1}{k_n^2}e^{-k_n x}\sin k_n y - \frac{2}{\pi}\int_0^\infty \left(t - \frac{\sin\beta t}{\beta}\right)\frac{\cosh k(y+1)}{\cosh k}\cos kx\,\frac{dk}{k^2}. \tag{30}$$

The vertical velocity of the fluid on the free surface, or the left-hand-side of (19), becomes

$$\phi_{1y} = \frac{2}{\pi}\int_0^\infty \frac{\sin\beta t}{\beta}\tanh k \cos kx\,\frac{dk}{k}, \tag{31}$$

where the logarithmic term arising from the infinite series has been cancelled with the help of (25). The free-surface elevation obtained by using (19) is

$$\eta = \frac{2\alpha}{\pi}\int_0^\infty \frac{1-\cos\beta t}{k^2(1+Tk^2)}\cos kx\,dk + O(\alpha^2) \tag{32}$$

when $\kappa = 0$. For non-zero κ and κ', but with $\kappa''' = 0$, a term

$$\frac{2\alpha T}{\pi}\int_0^\infty \left(\kappa - \kappa'\frac{\sin\beta t}{\beta}\right)\frac{\cos kx}{1+Tk^2}\,dk$$

would have to be added to the right-hand side of (32).

We can recover the small-time solution by rewriting (32) as the sum of an integral from zero to K and an integral from K to infinity, with K chosen such that $1 \ll K \ll (1/t^2)$. For $0 \leqslant k \leqslant K$, $\cos\beta t$ can be expanded in a Taylor series in time, whereas for $K \leqslant k < \infty$ we have $\tanh k = 1 + O(e^{-k})$. Then, in the absence of surface tension ($T = 0$), (32) can be expanded as $t \to 0$ with x fixed to give

$$\eta = -\frac{\alpha t^2}{\pi}\ln(\tanh\tfrac{1}{4}\pi x) + \frac{\alpha t^4}{24}\frac{x}{\sinh\tfrac{1}{2}\pi x} + \frac{\alpha t^6}{360\pi}\left[-\frac{1}{x^2} + \int_0^\infty k(\tanh^3 k - 1)\cos kx\,dk\right] + \dots. \tag{33}$$

The first term in (33) is consistent with the small-time solution of Peregrine (1972) and Chwang (1983), and the additional terms can be obtained by extending their small-time expansion to $O(\alpha t^6)$.

If both x and t are small, with $x = O(t^2)$, the integral (32) can be simplified when $T = 0$ by the addition and subtraction of $\frac{1}{2}kt^2\tanh k$ in the numerator of the integrand. The logarithmic term is obtained explicitly by the use of (25), and the remaining integral is written in two parts as before. It is found that

$$\eta = -\frac{\alpha t^2}{\pi}\ln\tfrac{1}{4}\pi x - \frac{2\alpha t^2}{\pi}\int_0^\infty \left(\frac{1}{2} - \frac{1-\cos k^{\frac{1}{2}}t}{kt^2}\right)\cos kx\,\frac{dk}{k} + \dots \tag{34}$$

(Joo, Messiter & Schultz 1988), where the integral is a function of x/t^2. Using integration by parts, we find the largest term to be $t^4/(720x^2)$ as $x/t^2 \to \infty$, which

agrees with the expansion of (33) as $x \to 0$. The velocity components can be found in a similar way. In complex form, with $z = x + iy = O(t^2)$ as $t \to 0$,

$$\phi_x - i\phi_y = i\frac{2\alpha t}{\pi}\left[\ln \tfrac{1}{4}\pi z + \int_0^\infty \left(\frac{1}{k} - \frac{\sin k^{\frac{1}{2}}t}{k^{\frac{3}{2}}t}\right)e^{-ikz}\,dk\right] + \dots. \tag{35}$$

This result can, of course, be obtained directly by replacing $\tanh{(\tfrac{1}{4}\pi x)}$ with $\tfrac{1}{4}\pi x$ in (19); the differential equation (24) for A then has $\cosh k$ replaced by 1 and $\sinh k$ by k.

The behaviour of the local solution obtained as $z/t^2 \to 0$ is more complicated. To expand the integral in (35) it is convenient to evaluate the following two integrals separately:

$$I_1 = \int_0^\infty \left[(e^{-ikz} - 1) + \left(1 - \frac{\sin k^{\frac{1}{2}}t}{k^{\frac{1}{2}}t}\right)\right]\frac{dk}{k},$$

$$I_2 = -\int_0^\infty (e^{-ikz} - 1)\frac{\sin k^{\frac{1}{2}}t}{k^{\frac{3}{2}}t}\,dk.$$

The integral I_1 contains a term that cancels the logarithmic term in (35). In I_2, repeated integration by parts provides a power series in z/t^2. Another kind of term appears when $k^{\frac{1}{2}}t$ and kz are both large and of the same order. This contribution is found by changing the integration contour and choosing the path of steepest descent from $k = t^2/(4z^2)$. Substituting these approximations into (35) finally gives

$$\phi_x - i\phi_y = \alpha t + i\frac{2\alpha t}{\pi}(\ln \tfrac{1}{4}\pi t^2 + \gamma - 2) - \frac{4\alpha t}{\pi}\left[\frac{z}{t^2} + i\left(\frac{z}{t^2}\right)^2 + \dots\right]$$

$$- \left[\frac{8\alpha t}{\pi^{\frac{1}{2}}}\left(\frac{z}{t^2}\right)^{\frac{3}{2}}\exp\left\{i\left(\frac{t^2}{4z} - \frac{\pi}{4}\right)\right\} + \dots\right] + \dots, \tag{36}$$

for $t \to 0$ and $z/t^2 \to 0$, where $\gamma = 0.577\dots$ is the Euler constant. The corresponding local solution for the surface elevation is

$$\eta = -\frac{\alpha t^2}{\pi}\left[(\ln \tfrac{1}{4}\pi t^2 + \gamma - 3) + \pi\left(\frac{x}{t^2}\right) + 2\left(\frac{x}{t^2}\right)^2 + \dots\right]$$

$$- \frac{16\alpha t^2}{\pi^{\frac{1}{2}}}\left(\frac{x}{t^2}\right)^{\frac{5}{2}}\cos\left(\frac{t^2}{4x} - \frac{\pi}{4}\right) + \dots + O(\alpha^2). \tag{37}$$

This result is identical to that of Roberts (1987) except that the term $\ln{(\tfrac{1}{4}\pi t^2)}$ replaces $\ln t^2$. This discrepancy is due to the difference in the problems: Roberts (1987) considered an infinitely deep fluid with a finite-depth wavemaker, $-1 < y < 0$. Thus when $T = 0$ the form of the surface elevation for small time and near the wavemaker depends on the similarity variable x/t^2 as $x \to 0$ and $t \to 0$. For example, equations (33) and (37) show different behaviour for η at large and small values of x/t^2.

One important implication of (32) concerns the slope of the free surface very near the contact line. As $T \to 0$ it is obvious from (20) that a singular-perturbation problem arises near the contact line. The solution to this problem can be recovered from (32). Differentiation of (32) with respect to x and introduction of the transformation $\tilde{k} = kx$ yields

$$\eta_{1x} = -\frac{2}{\pi}\int_0^\infty \left\{1 - \cos\left(\left[\tilde{k}\left(1 + T\frac{\tilde{k}^2}{x^2}\right)\right]^{\frac{1}{2}}\frac{t}{x^{\frac{1}{2}}}\right)\right\}\frac{\sin \tilde{k}\,d\tilde{k}}{\tilde{k}\left(1 + T\dfrac{\tilde{k}^2}{x^2}\right)},$$
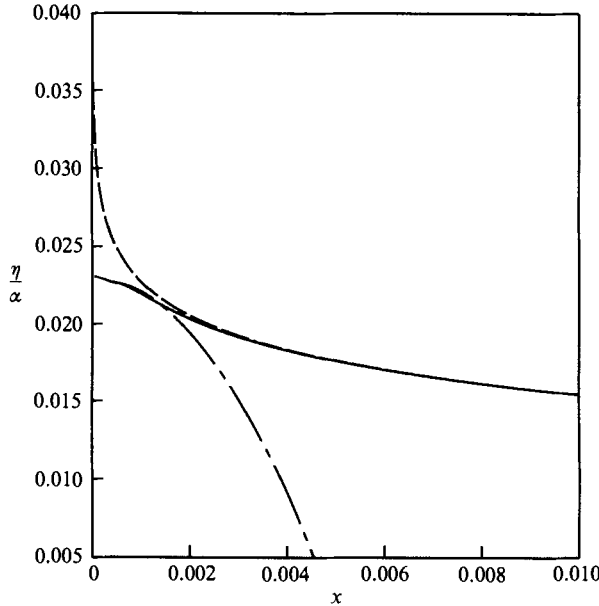
FIGURE 2. Free-surface elevations for the ramp velocity at $t = 0.1$ according to present method
(——) and compared to the small-time solution (———) and the local solution (— — —).

where the tanh k factor has been replaced by 1 for small x, since the contribution for small k is negligible. Now if $x/t^2 \to 0$, the cosine term in the integrand oscillates rapidly, and the contribution of this term to the integral is small. The remaining term can be integrated to give

$$\eta_x = (\alpha - \kappa_0)\exp\left(-\frac{x}{T^{\frac{1}{2}}}\right) - \alpha + O(\alpha^2), \tag{38}$$

as $x/t^2 \to 0$ and $T \to 0$ with $x/T^{\frac{1}{2}}$ fixed. Thus, the dynamic contact angle approaches the static contact angle for $T \neq 0$ as prescribed. However, when the surface tension is zero, (38) becomes $\eta_x = -\alpha$ as $x \to 0$ in agreement with (37). This also agrees with Roberts' (1987) findings and implies a jump in the contact angle at $t = 0$ if T is neglected. For small but non-zero T, the discrepancy is explained by the large curvature $\eta_{xx} = \kappa_0/T^{\frac{1}{2}}$ at $x = 0$, as shown by (38).

The integral in (32) is evaluated numerically as the sum of integrals from zero to M and M to infinity. The value for M is chosen to be as large as 10^5 for small x and t, and as small as 10^{-1} when either x or t is large. The integral from zero to M is evaluated using 10-point Gauss–Legendre and 21-point Kronrod formulae on both halves of the adaptive subintervals. The selection of the subinterval is based on the maximum absolute error estimate of 10^{-9}. Owing to the rapid oscillation of the integrand, the integral from M to infinity is obtained using Filon's method.

Comparisons of (32) with the small-time solution and the local solution are illustrated in figure 2. For small time ($t = 0.1$) and $T = 0$, (32) agrees with the local solution (37) near the wall ($x \ll t^2$), and with the small-time solution (33) sufficiently far from the wall. Figure 3 shows the free-surface configuration at small time for two different scales when κ_0 is zero. A numerical value of the non-dimensional surface tension, T, for pure water at 70 °F with an undisturbed depth of 1 ft is approximately
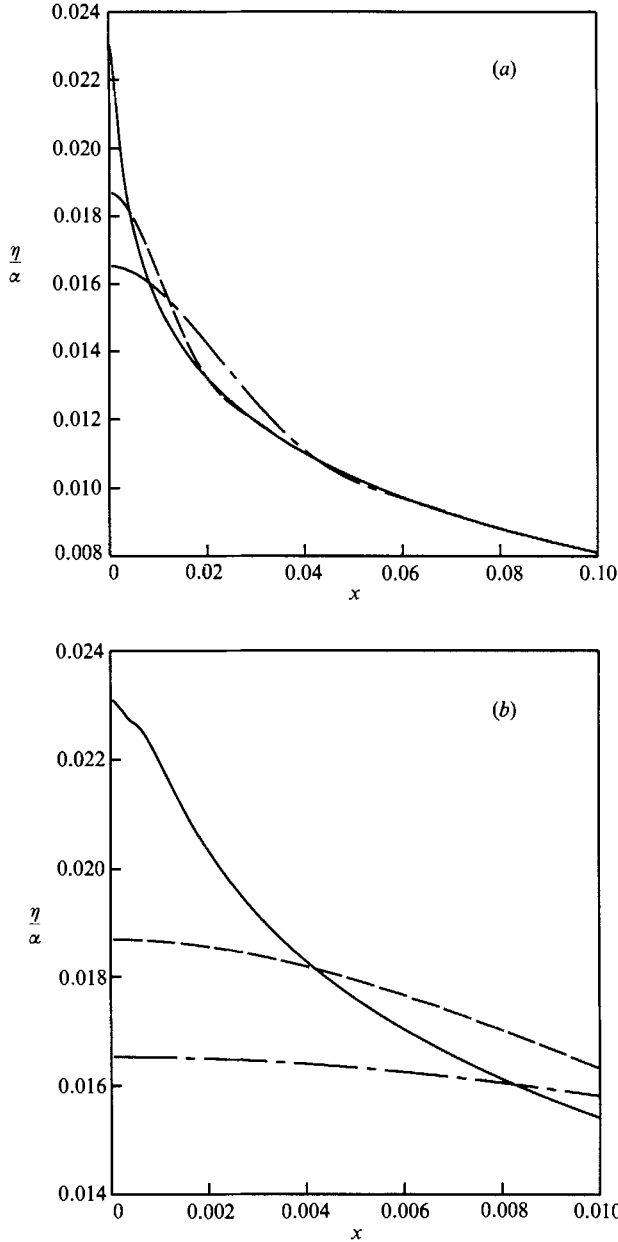
FIGURE 3. Free-surface elevations for the ramp velocity at $t = 0.1$ when surface tension $T = 0$ (——), $T = 10^{-4}$ (– – –), and $T = 10^{-3}$ (— — —): (a) large x/t^2; (b) small x/t^2.

0.8×10^{-4}, represented by $T = 10^{-4}$ in figure 3. When the surface tension is zero, small-scale waves (or wiggles) can be observed very near the wall, as also noted by Roberts (1987). These wiggles are suppressed in the presence of surface tension, in which case the static contact angle (90° in this case) is retained. At a given time, surface tension also decreases the contact-line elevation. Far from the wavemaker the effect of surface tension becomes less important. These effects become more obvious as we proceed to a step velocity.

4. Step velocity

The wavemaker velocity given by (3) when $q = 0$ is a step velocity, i.e. the wavemaker initially at rest is suddenly set in motion at $t = 0^+$ with a constant velocity.

When the velocity of the wall C is small compared with $(gh)^{\frac{1}{2}}$, the expansions in (9) and (10) for small Froude number can be used as before. This time, the Froude number α and the dimensionless velocity $u(t)$ are given as

$$\alpha = \frac{C}{(gh)^{\frac{1}{2}}} \quad \text{and} \quad u(t) = 1. \tag{39}$$

With $u(t) = 1$, the solution to (24) with the initial conditions in (27) is

$$A(k, t) = -\frac{2}{\pi} \frac{1}{k} \frac{1}{\cosh k} (1 - \cos \beta t). \tag{40}$$

From (16) and (22),

$$\phi_1 = 2 \sum_{n=0}^{\infty} \frac{1}{k_n^2} e^{-k_n x} \sin k_n y - \frac{2}{\pi} \int_0^{\infty} (1 - \cos \beta t) \frac{\cosh k(y+1)}{\cosh k} \cos kx \frac{dk}{k^2}. \tag{41}$$

After cancellation of the logarithmic terms, the vertical velocity of the free surface becomes

$$\phi_{1y} = \frac{2}{\pi} \int_0^{\infty} \cos \beta t \tanh k \cos kx \frac{dk}{k}. \tag{42}$$

Equation (19) then gives the free-surface elevation for $\kappa_0 = 0$ as

$$\eta = \frac{2\alpha}{\pi} \int_0^{\infty} \frac{\beta \sin \beta t}{k^2(1 + Tk^2)} \cos kx \, dk + O(\alpha^2). \tag{43}$$

It is interesting to note that, since the problem is linear, (42) and (43) can be derived directly by differentiating (31) and (32) with respect to time. This procedure is related to Roberts' (1987) use of a convolution integral.

As in the case of a ramp velocity, (43) with $T = 0$ can be shown to agree with

$$\eta = -\frac{2\alpha t}{\pi} \ln (\tanh \tfrac{1}{4}\pi x) + O(\alpha t^3)$$

sufficiently far from the wall, for $x \gg t^2$, and with

$$\eta = -\frac{2\alpha t}{\pi} \left[(\ln \tfrac{1}{4}\pi t^2 + \gamma - 2) - 2 \left(\frac{x}{t^2} \right)^2 + \ldots \right] + \frac{8\alpha t}{\pi^{\frac{1}{2}}} \left(\frac{x}{t^2} \right)^{\frac{3}{2}} \sin \left(\frac{t^2}{4x} - \frac{\pi}{4} \right)$$

$$+ \frac{48\alpha t}{\pi^{\frac{1}{2}}} \left(\frac{x}{t^2} \right)^{\frac{5}{2}} \cos \left(\frac{t^2}{4x} - \frac{\pi}{4} \right) + \ldots + O(\alpha^2)$$

near the contact line, for $x \ll t^2$. These equations, the small-time solution and the local solution, can be obtained either by tedious analysis or by direct time-differentiation of (33) and (37). Again it is evident that as $x \to 0$ and $t \to 0$ the solution for η depends on the path of approach to the origin in the (x, t)-plane.

If (43) is rewritten when $T = 0$ in terms of $\tilde{k} = kx$, it can be shown that $\eta_x = O(\alpha/x^{\frac{1}{2}})$ as $t, x \to 0$ with x/t^2 fixed. This behaviour of η_x is also implied by the

expansions for large and small x/t^2. However, since the asymptotic representation requires $|\eta_x| \ll 1$, and therefore $x \gg \alpha^2$, a different inner solution is needed for $t = O(\alpha)$, $x = O(\alpha^2)$. The same conclusion can also be anticipated from dimensional considerations. The relevant parameters for points near the contact line at small time should be C and g rather than g and h, so that the proper reference length and time are $C^2/g = \alpha^2 h$ and $C/g = \alpha(h/g)^{\frac{1}{2}}$, respectively. The corresponding coordinates are t/α and x/α^2.

The correct formulation of an inner problem for small t and x can be shown to require the full nonlinear free-surface conditions. The proper asymptotic form is inferred from the condition that the inner solutions for η, ϕ_x, ϕ_y match with expansions of the previous solutions obtained from (41) and (43) as $x, y, t \to 0$. When (43) is replaced by a representation analogous to (34), it is seen that the largest term in the inner solution for η must match with a term $O(\alpha t \ln \alpha)$. The corresponding y-coordinate should be measured from this first approximation to the surface elevation. Matching the velocities implies that $\phi_x = O(\alpha)$ and $\phi_y = O(\alpha \ln \alpha)$ in the small-scale solution. Finally, the dynamic boundary condition implies $\phi_t = O(\alpha^2 \ln^2 \alpha)$.

The above considerations suggest that sufficient generality may be achieved with a solution of the form

$$\phi = (\alpha^3 \ln^2 \alpha)\,\hat{\phi}_1(\hat{t}) + (\alpha^3 \ln \alpha)\,\hat{\phi}_2(\hat{x}, \hat{y}, \hat{t}) + \alpha^3 \hat{\phi}_3(\hat{x}, \hat{y}, \hat{t}) + \dots, \tag{44}$$

$$\eta = (\alpha^2 \ln \alpha)\,\hat{\eta}_1(\hat{t}) + \alpha^2 \hat{\eta}_2(\hat{x}, \hat{t}) + \dots, \tag{45}$$

where
$$\hat{x} = \frac{x}{\alpha^2}, \quad \hat{y} = \frac{y - (\alpha^2 \ln \alpha)\,\hat{\eta}_1(\hat{x}, \hat{t})}{\alpha^2}, \quad \hat{t} = \frac{t}{\alpha}.$$

Matching gives $\hat{\phi}_{2\hat{x}} \to 0$ and $\hat{\phi}_{2\hat{y}} \to -4/\pi$ as $\hat{x} \to \infty$; since the complex velocity $\hat{\phi}_{2\hat{x}} - i\hat{\phi}_{2\hat{y}}$ is bounded everywhere, it is constant. Terms $O(\alpha^2 \ln^2 \alpha)$ in (5) then give $\hat{\phi}_{1\hat{t}} - \hat{\eta}_{1\hat{t}}\hat{\phi}_{2\hat{y}} + \frac{1}{2}\hat{\phi}_{2\hat{y}}^2 = 0$, where $\hat{\phi}_{2\hat{y}} = -4/\pi$; the kinematic condition (4) shows that $\hat{\eta}_{1\hat{t}} = -4/\pi$. Finally, it follows from (5) that $\hat{\phi}_{2\hat{t}} = -\hat{\eta}_1$. The expansions (44) and (45) therefore become

$$\phi = (\alpha^3 \ln^2 \alpha)\frac{8\hat{t}}{\pi^2} - 2(\alpha^3 \ln \alpha)\left(\frac{2\hat{y}}{\pi} - \frac{\hat{t}^2}{\pi}\right) + \alpha^3 \hat{\phi}_3(\hat{x}, \hat{y}, \hat{t}) + \dots, \tag{46}$$

$$\eta = -(\alpha^2 \ln \alpha)\frac{4\hat{t}}{\pi} + \alpha^2 \hat{\eta}_2(\hat{x}, \hat{t}) + \dots. \tag{47}$$

Conditions to be satisfied by $\hat{\phi}_3$ and $\hat{\eta}_2$ at $\hat{y} = \hat{\eta}_2$ are determined from (4) and (5):

$$\hat{\phi}_{3\hat{t}} + \hat{\eta}_2 + \tfrac{1}{2}(\hat{\phi}_{3\hat{x}}^2 + \hat{\phi}_{3\hat{y}}^2) = 0, \tag{48}$$

$$\hat{\phi}_{3\hat{y}} - \hat{\eta}_{2\hat{t}} - \hat{\phi}_{3\hat{x}}\hat{\eta}_{2\hat{x}} = 0. \tag{49}$$

That is, for the wavemaker with a step velocity, the full nonlinear free-surface conditions are required for $\hat{\phi}_3$ and $\hat{\eta}_2$ and are to be evaluated at the unknown location $\hat{y} = \hat{\eta}_2$. The condition (2) at the wavemaker leads to

$$\hat{\phi}_{3\hat{x}} = 1$$

and is to be evaluated at the actual location of the wall $\hat{x} = \hat{t}$. Thus, the linearized formulation for small Froude number α fails when $t = O(\alpha)$ and $x = O(\alpha^2)$. Here, a full nonlinear problem must be solved, with some added terms involving $\ln \alpha$.

The large-time behaviour of the fluid motion is also of interest. The free-surface

configuration for large time, but still $t \ll (1/\alpha)$, can be obtained by an asymptotic evaluation of (43). If $\eta = 0$ initially ($\kappa_0 = 0$), the free-surface elevation (43) can be written as

$$\eta = \frac{\alpha}{\pi} \int_0^\infty \sin(\beta t - kx) \frac{\beta\, \mathrm{d}k}{k^2(1+Tk^2)} + \frac{\alpha}{\pi} \int_0^\infty \sin(\beta t + kx) \frac{\beta\, \mathrm{d}k}{k^2(1+Tk^2)} + O(\alpha^2). \quad (50)$$

As $t \to \infty$, the largest contribution to the integrals occurs for small k, at $k = O\{1/(t-x)\}$. If x is not close to t, it is sufficient for a first approximation to replace β by k in the integrand and to omit Tk^2 in the denominator. The result equals α for $x < t$ and zero for $x > t$ (recall that $\mathrm{d}x/\mathrm{d}t = 1$ corresponds to the speed $(gh)^{\frac{1}{2}}$ of a shallow-water wave). This approximation, however, neglects $(k-\beta)t \ll k|t-x|$ and therefore fails near the wave front, $x = t$; i.e. since $k-\beta \sim \frac{1}{6}(1-3T)k^3$ and $k = O\{1/(t-x)\}$, it has been assumed that $|t-x|^3 \ll t$. When $t-x = O(t^{\frac{1}{3}})$, the cubic term in k must be retained, and the surface elevation becomes

$$\eta = \alpha \int_\lambda^\infty \mathrm{Ai}(\xi)\, \mathrm{d}\xi + \dots, \quad (51)$$

where $\lambda = (1-3T)^{-\frac{1}{3}}(2/t)^{\frac{1}{3}}(x-t)$ and Ai is the Airy function. For $\lambda > 0$ and $x-t \gg t^{\frac{1}{3}}$, η is exponentially small; for $\lambda < 0$ and $t^{\frac{1}{3}} \ll t-x \ll t$,

$$\eta = \alpha - \frac{\alpha}{(\pi t)^{\frac{1}{2}}} \left(\frac{1-3T}{2}\right)^{\frac{1}{4}} \left(1-\frac{x}{t}\right)^{-\frac{3}{4}} \cos\left[\frac{2}{3}\left(\frac{2}{1-3T}\right)^{\frac{1}{2}} t\left(1-\frac{x}{t}\right)^{\frac{3}{2}} + \frac{\pi}{4}\right] + \dots. \quad (52)$$

When $t-x = O(t)$ behind the wave front, the first integral in (50) has a stationary point at $k = O(1)$ and contributes a term $O(\alpha t^{-\frac{1}{2}})$ that matches with (52). In the second integral there is no stationary point when $x > 0$, and the integration contour can be deformed to lie somewhat away from the real axis in the complex k-plane. The largest contribution is near $k = 0$, giving the value $\frac{1}{2}\pi$ with exponentially small error.

Therefore, as time becomes large, the contact-line elevation approaches a value equal to the Froude number, and behind the wave front the free surface can be approximated by a wavetrain superimposed on a flat surface of the same height as the contact line. The amplitude of this wavetrain is $O(\alpha t^{-\frac{1}{2}})$, increasing to $O(\alpha)$ near the wave front. Surface tension increases the frequency and decreases the amplitude decay rate of the wavetrain. Beyond the wave front the free-surface elevation decreases exponentially to the undisturbed value of zero. The width of the wave front increases in proportion to $t^{\frac{1}{3}}$, so that the slope of the free surface near $x = t$ is $O(\alpha t^{-\frac{1}{3}})$.

In figure 4, the free-surface elevation is shown at several different times for zero initial elevation ($\kappa_0 = 0$) and for three values of the non-dimensional surface tension; similar curves have been given by Roberts (1987) for $T = 0$. Near the wavemaker ($x \ll t^2$), the free surface is made up of an infinite number of wiggles, which can be approximated by a local solution. The singular behaviour of the surface slope η_x at $x = 0$ is not visible in figure 4 because the amplitude of the oscillation approaches zero as $x \to 0$. Surface tension suppresses the wiggles, but the effects of surface tension are seen to decrease as the distance from the wavemaker increases. This explains why the agreement with experimental measurements (Dommermuth *et al.* 1988) is good even though surface tension is neglected at moderate distances from the wavemaker. Also shown in figure 4(*e*) is the asymptotic solution (51) evaluated using the Taylor series and the asymptotic representations in Abramowitz & Stegun (1965), which is in good agreement with the numerical evaluation of exact solution (43) near the wave front. Figure 4(*b*) shows the solution at very small x; if specific non-vanishing small
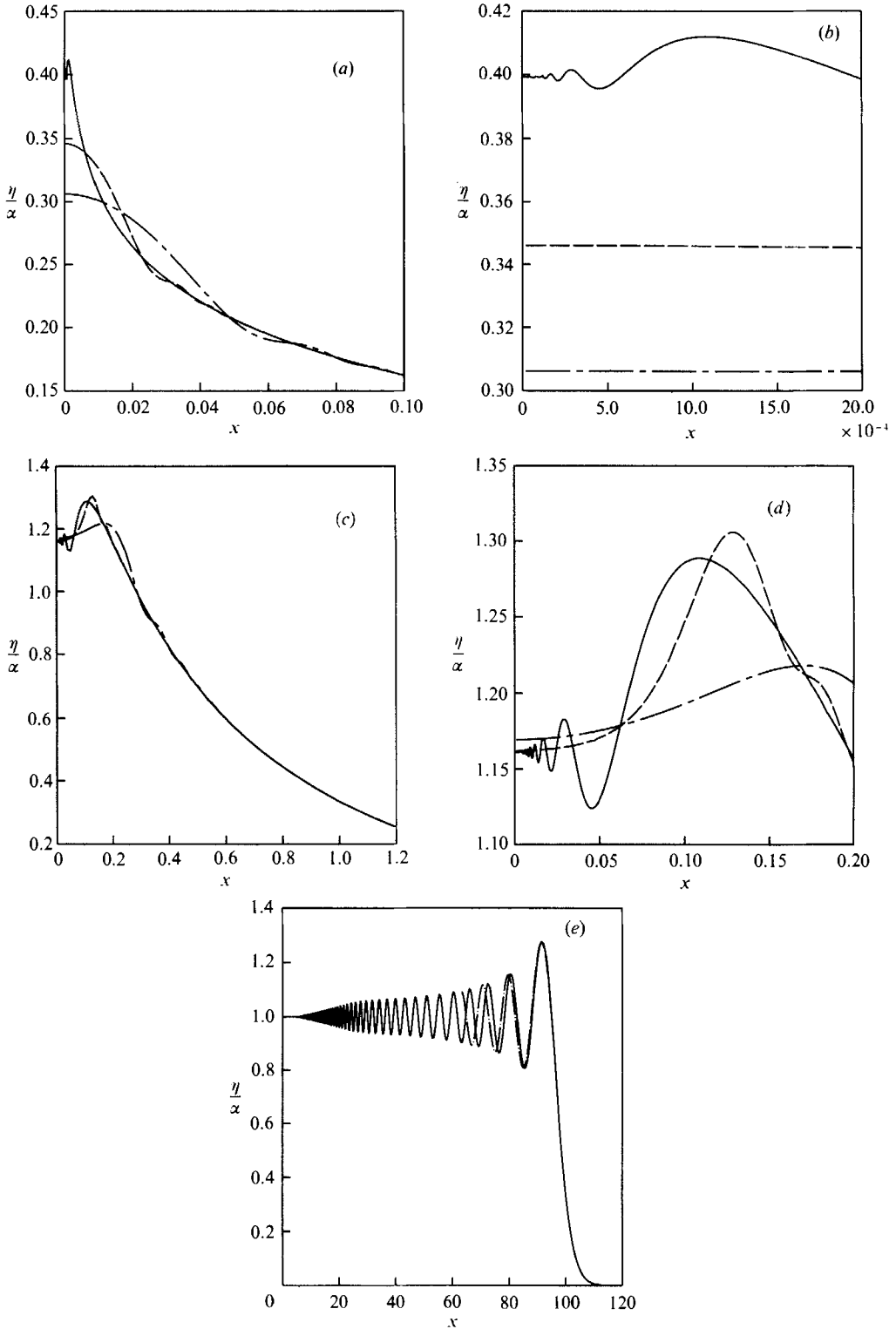
FIGURE 4. Free-surface elevations for the step velocity when surface tension $T = 0$ (———), $T = 10^{-4}$ (---), and $T = 10^{-3}$ (————): (*a*) $t = 0.1$; (*b*) $t = 0.1$, $x \ll t^2$; (*c*) $t = 1$; (*d*) $t = 1$, $x \ll t$; (*e*) $t = 100$ with the asymptotic solution near the wave front (—·—).
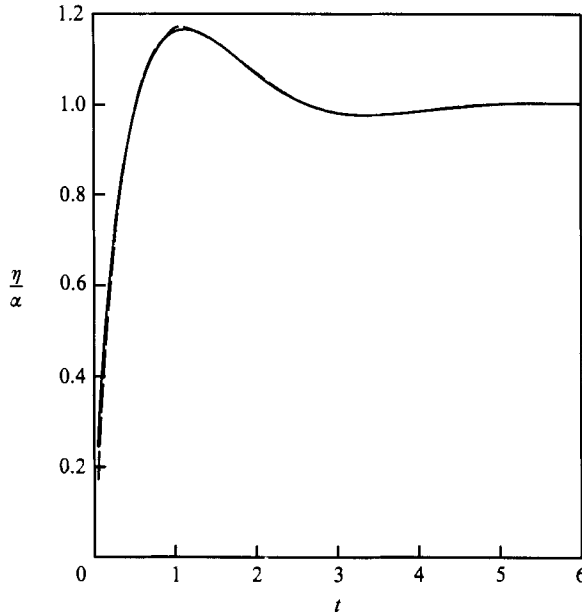
FIGURE 5. Contact-line elevation for the step velocity when surface tension $T = 0$ (———)
and $T = 10^{-3}$ (– – –).

values of α are chosen, the coordinate x should be regarded as measured from the wavemaker surface as discussed in §2.

The distance from the wavemaker occupied by the wiggles increases with time in agreement with the local solution. The contact-line elevation increases to a maximum, and then oscillates to converge to the Froude number at large time (figure 5). Figure 4(d) shows that for certain values of time the surface tension actually makes the contact-line elevation higher, as also shown in figure 5. The amplitude and frequency of the wiggles near the wavemaker decrease with time until the free surface becomes flat, as indicated by the analysis (50)–(52).

5. Exponential wavemaker velocity

As a general example that includes the step and ramp velocities as limiting cases, we consider a wavemaker velocity that has a finite jump in acceleration at $t = 0$ and approaches a constant value U_0 as $t \to \infty$. The exponential form

$$U(t) = U_0\left\{1 - \exp\left[-\left(\frac{h}{g}\right)^{\frac{1}{2}}\frac{t}{\tau}\right]\right\}, \tag{53}$$

where τ is a characteristic time, exhibits this behaviour. The limits $\tau \to 0$ and $\tau \to \infty$ correspond to the step velocity and the ramp velocity, respectively. The expansions for small Froude number, (9) and (10), are applied with

$$\alpha = \frac{U_0}{(gh)^{\frac{1}{2}}} \quad \text{and} \quad u(t) = 1 - e^{-bt}, \tag{54}$$

as the Froude number and non-dimensional velocity, respectively. Here $b = [h/(g\tau^2)]^{\frac{1}{4}}$. Now, (24) and (27) give

$$A(k,t) = -\frac{2}{\pi}\frac{1}{k^2\cosh k}\left(1 - \cos\beta t - \beta\frac{\beta\,\mathrm{e}^{-bt} + b\sin\beta t - \beta\cos\beta t}{b^2 + \beta^2}\right). \qquad (55)$$

Equations (16) and (22) then give the first-order velocity potential as

$$\phi_1 = 2(1 - \mathrm{e}^{-bt})\sum_{n=0}^{\infty}\frac{1}{k_n^2}\mathrm{e}^{-k_n x}\sin k_n y - \frac{2}{\pi}\int_0^{\infty}\frac{\cosh k(y+1)}{\cosh k}\cos kx$$

$$\times\left(1 - \cos\beta t - \beta\frac{\beta\,\mathrm{e}^{-bt} + b\sin\beta t - \beta\cos\beta t}{b^2 + \beta^2}\right)\frac{\mathrm{d}k}{k^2}. \qquad (56)$$

The vertical velocity on the free surface, after cancellation of the singular terms, becomes

$$\phi_{1y} = \frac{2}{\pi}\int_0^{\infty}\cos\beta t\tanh k\cos kx\frac{\mathrm{d}k}{k} - \frac{2}{\pi}\int_0^{\infty}\frac{b^2\,\mathrm{e}^{-bt} - \beta b\sin\beta t + \beta^2\cos\beta t}{b^2 + \beta^2}\tanh k\cos kx\frac{\mathrm{d}k}{k}, \qquad (57)$$

and the free-surface elevation becomes, for $\kappa = 0$,

$$\eta = \frac{2\alpha}{\pi}\int_0^{\infty}\frac{\beta\sin\beta t}{k^2(1 + Tk^2)}\cos kx\,\mathrm{d}k + \frac{2\alpha}{\pi}\int_0^{\infty}\frac{b\,\mathrm{e}^{-bt} - b\cos\beta t - \beta\sin\beta t}{b^2 + \beta^2}\tanh k\cos kx\frac{\mathrm{d}k}{k} + O(\alpha^2). \qquad (58)$$

With t fixed, if $b \to 0$, (58) approaches the solution (32) for the ramp velocity with α replaced by αb; if $b \to \infty$, it approaches the solution (43) for the step velocity. The first term in (58) is identical to that for the step velocity, and the other term decays to zero as $t \to \infty$. Consequently, as $t \to \infty$ the behaviour of the fluid eventually follows that of the step velocity regardless of the startup process. As $t \to 0$ a special case arises when $b \to \infty$ such that bt becomes constant in the limit – the solution then depends on the value of bt. If $bt \to 0$ or $bt \to \infty$, as $t \to 0$, the small-time solution is recovered for the ramp and the step velocity, respectively.

As discussed in §2, we have prescribed $\kappa = 0$ here, so that the contact angle remains unchanged from its initial static state in the presence of surface tension. We now examine the relationship between the acceleration of the wavemaker and the surface slope at $x = 0$ when the capillary effect is absent. When the surface tension is zero $(T = 0)$, differentiation of (58) with respect to x and the transformation $\tilde{k} = kx$ yield

$$\eta_x = -\frac{2\alpha}{\pi}\int_0^{\infty}\left(1 - \frac{\tilde{k}\tanh(\tilde{k}/x)}{xb^2 + \tilde{k}\tanh(\tilde{k}/x)}\right)(\tilde{k}\tanh(\tilde{k}/x))^{\frac{1}{2}}\sin\left[(\tilde{k}\tanh(\tilde{k}/x))^{\frac{1}{2}}\frac{t}{x^{\frac{1}{2}}}\right]\sin\tilde{k}\frac{\mathrm{d}\tilde{k}}{k}$$

$$-\frac{2\alpha b}{\pi}\int_0^{\infty}\left\{\mathrm{e}^{-bt} - \cos\left[\left(\tilde{k}\tanh\frac{\tilde{k}}{x}\right)^{\frac{1}{2}}\frac{t}{x^{\frac{1}{2}}}\right]\right\}\frac{\tanh(\tilde{k}/x)}{xb^2 + \tilde{k}\tanh(\tilde{k}/x)}\sin\tilde{k}\,\mathrm{d}\tilde{k} + O(\alpha^2). \qquad (59)$$

When $x \to 0$ and $x/t^2 \to 0$, this can be evaluated as

$$\eta_x = -\alpha b\,\mathrm{e}^{-bt} + \dots. \qquad (60)$$

Therefore, the slope of the free surface very near the contact line jumps instantaneously to a finite value, which depends on the Froude number and the exponent b, and decays to zero again as time becomes large. If b is large, an additional
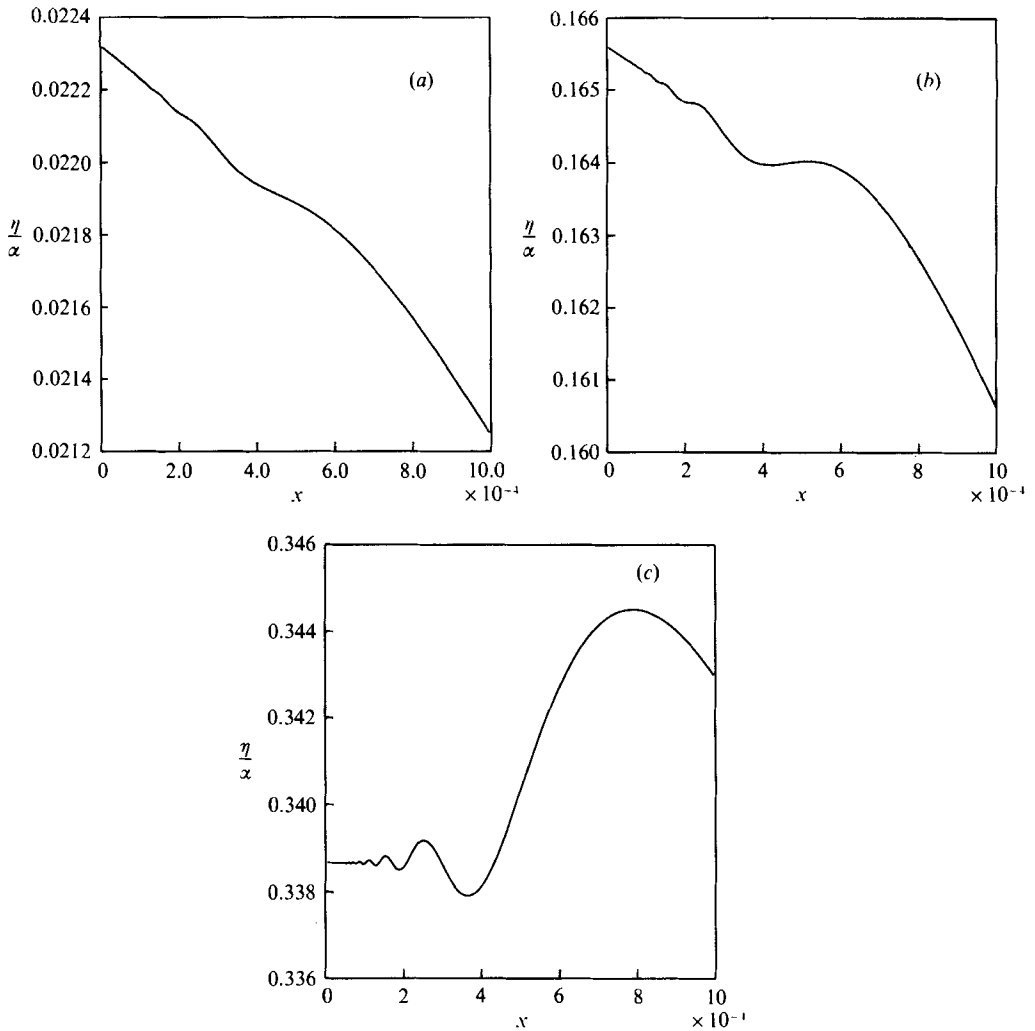
FIGURE 6. Free-surface elevations for the exponential velocity at $t = 0.1$ when surface tension $T = 0$: (a) $b = 1$; (b) $b = 10$; (c) $b = 50$.

term $O(\alpha/x^{\frac{1}{2}})$ appears in the expansion of (59). For the step velocity, the correct surface slope near $x = 0$ would be recovered (for $1/b \ll t \ll 1$) only if the additional term were retained. On the other hand, (60) does remain correct if b is small, giving a surface slope near $x = 0$ that is consistent with the previous result for the ramp velocity, if the difference in definition of the Froude numbers is taken into account.

As shown in the previous section, the linear solution for the step velocity is not valid for very small time, and a fully nonlinear formulation is required. This can be more easily understood by examining the limitation to be imposed on the time constant (or b) for the present wavemaker if the linear solution is to be valid. As we proceed to the next order, $O(\alpha^2)$, terms proportional to $\alpha^2 b\,e^{-bt}$ will appear. Then, for $b \gg 1$ the expansions (9) and (10) are valid for all time, including $t \ll (1/b)$ only when $b \ll (1/\alpha)$. If $b = O(1/\alpha)$, nonlinear terms are required when $bt = O(1)$. Therefore, the nonlinear effects cannot be neglected for a rapidly accelerated wavemaker ($\tau = O(U_0/g)$). This is also consistent with (60) when it is combined with the kinematic

boundary condition on the free surface (4), which gives the same criterion for the validity of linearization as above.

The free-surface configurations for various values of b are shown in figure 6 when surface tension and initial free-surface elevation are absent. They resemble those for the ramp velocity when b is small, and those for the step velocity when b is large. As the acceleration of the wavemaker increases (as b becomes larger), the amplitude of the wiggles grows and the contact angle approaches $90°$, which is consistent with the above analysis.

6. Harmonic wavemaker velocity

6.1. Simple-harmonic motion

A wavemaker motion of greater practical interest is the periodic oscillation, for which the velocity of the wall is given as

$$U(t) = U_0 \sin\left[\left(\frac{h}{g}\right)^{\frac{1}{2}} \Omega t\right], \quad t > 0, \tag{61}$$

where U_0 is the maximum velocity of the wall and Ω is the frequency of the oscillation. The well-known linear steady-state solution to this problem was obtained by Havelock (1929) and has been extended by many others. The Fourier-integral method adopted in this study will lead to a transient solution that agrees with the steady-state solution as $t \to \infty$.

The Froude number is defined as in the previous section, and the normalization of the wavemaker velocity gives

$$u(t) = \sin \omega t, \tag{62}$$

where the non-dimensional frequency of the wavemaker oscillation is $\omega = \Omega(h/g)^{\frac{1}{2}}$, so the solution for (24) that satisfies (27) is now

$$A(k,t) = \frac{2}{\pi} \frac{\beta}{k^2 \cosh k} \frac{\beta \sin \omega t - \omega \sin \beta t}{\omega^2 - \beta^2}. \tag{63}$$

Therefore, the complete first-order velocity potential is

$$\phi_1 = 2 \sin \omega t \sum_{n=0}^{\infty} \frac{1}{k_n^2} e^{-k_n x} \sin k_n y + \frac{2}{\pi} \int_0^\infty \frac{\beta(\beta \sin \omega t - \omega \sin \beta t) \cosh k(y+1)}{(\omega^2 - \beta^2) \cosh k} \cos kx \frac{dk}{k^2}. \tag{64}$$

Again, the singular terms in the vertical velocity are cancelled to give

$$\phi_{1y} = \frac{2\omega}{\pi} \int_0^\infty \frac{\omega \sin \omega t - \beta \sin \beta t}{\omega^2 - \beta^2} \tanh k \cos kx \frac{dk}{k} \tag{65}$$

on the free surface. The free-surface elevation is then, for $\kappa = 0$,

$$\eta = \frac{2\alpha\omega}{\pi} \int_0^\infty \frac{\cos \omega t - \cos \beta t}{\beta^2 - \omega^2} \tanh k \cos kx \frac{dk}{k} + O(\alpha^2). \tag{66}$$

Far from the wavemaker, the asymptotic evaluation of (66) is possible in the limit as $t \to \infty$. As x and t become large, the largest contribution to the integral in (66) occurs in the neighbourhood of $k = k_0$, where k_0 is the positive real root of

$$k_0(1 + Tk_0^2) \tanh k_0 = \omega^2. \tag{67}$$

Since this is just the dispersion relation, k_0 is the wavenumber that would be observed for waves with a single frequency ω. Therefore, (66) can be written as

$$\eta = \frac{2\alpha\omega}{\pi}\int_{k_0-\epsilon}^{k_0+\epsilon}\frac{\cos\omega t\cos kx - \frac{1}{2}\cos(kx+\beta t) - \frac{1}{2}\cos(kx-\beta t)}{\beta^2-\omega^2}\tanh k\,\frac{\mathrm{d}k}{k}+\ldots, \quad (68)$$

where ϵ is a small number such that $1 \ll (1/\epsilon) \ll x$. The integrand in (68) can be expanded about $k = k_0$ and the resulting equation can be easily simplified after setting $(k-k_0)x = \bar{k}$:

$$\eta = \frac{\alpha\tanh k_0}{\pi k_0 C_{\mathrm{g}}}\int_0^\infty\left[-2\cos\omega t\sin k_0 x\,\frac{\sin\bar{k}}{\bar{k}}\right.$$
$$\left.+\sin(k_0 x+\omega t)\frac{\sin(1+C_{\mathrm{g}}t/x)\bar{k}}{\bar{k}}+\sin(k_0 x-\omega t)\frac{\sin(1-C_{\mathrm{g}}t/x)\bar{k}}{\bar{k}}\right]\mathrm{d}\bar{k}+\ldots. \quad (69)$$

Here, C_{g} is the group velocity of the gravity–capillary wave with wavenumber k_0 and is given by

$$C_{\mathrm{g}} = \frac{(1+3Tk_0^2)\,\omega^2+k_0^2(1+Tk_0^2)\,\mathrm{sech}^2\,k_0}{2k_0\,\omega}. \quad (70)$$

When $x > C_{\mathrm{g}}t$, the approximation (69) is zero; when $x < C_{\mathrm{g}}t$, (69) gives

$$\eta = -\frac{\alpha\tanh k_0}{k_0\,C_{\mathrm{g}}}\sin(k_0 x-\omega t)+\ldots, \quad (71)$$

which describes the free-surface configuration in a region behind the wave front but far ahead of the wavemaker. In the absence of surface tension ($T = 0$), the approximation (71) agrees with the steady-state solution away from the wavemaker obtained by Havelock (1929). As for the step velocity, the behaviour of the free surface near the wave front ($x = C_{\mathrm{g}}t$) could be obtained by extending the above analysis to higher orders.

The behaviour of the contact angle in the absence of surface tension is obtained by differentiating (66) with respect to x and transforming k to $\tilde{k}$ as before, which gives

$$\eta_x = -\frac{2\alpha\omega}{\pi}\int_0^\infty\left\{\cos\omega t-\cos\left[\left(\tilde{k}\tanh\frac{\tilde{k}}{x}\right)^{\frac{1}{2}}\frac{t}{x^{\frac{1}{2}}}\right]\right\}\frac{\tanh(\tilde{k}/x)}{\tilde{k}\tanh(\tilde{k}/x)-x\omega^2}\sin\tilde{k}x\,\mathrm{d}\tilde{k}+O(\alpha^2).$$

This can be simplified to
$$\eta_x = -\alpha\omega\cos\omega t+\ldots \quad (72)$$

as $x/t^2 \to 0$ and $x \to 0$. The discontinuity in the contact angle at $t = 0$ is consistent with the previous results. It can be easily observed from (72) that the contact angle oscillates with a 90° phase shift from the wavemaker velocity.

Figure 7 shows the free-surface configuration at large time for two different wavemaker frequencies. The harmonic wavetrain of Havelock (1929) is observed between the wavemaker and the harmonic-wave front, $x = C_{\mathrm{g}}t$. The amplitude and frequency of this wavetrain can be obtained easily from (67), (70) and (71). As the undisturbed free surface is approached, ahead of the harmonic-wave front, we observe a second wave front that travels at the maximum phase velocity $\mathrm{d}x/\mathrm{d}t = 1$, the value for shallow-water waves. The waves between these wave fronts are seen to have decreasing amplitude and wavenumber. The largest change of amplitude occurs near $x = C_{\mathrm{g}}t$ in both figures 7(a) and 7(b).
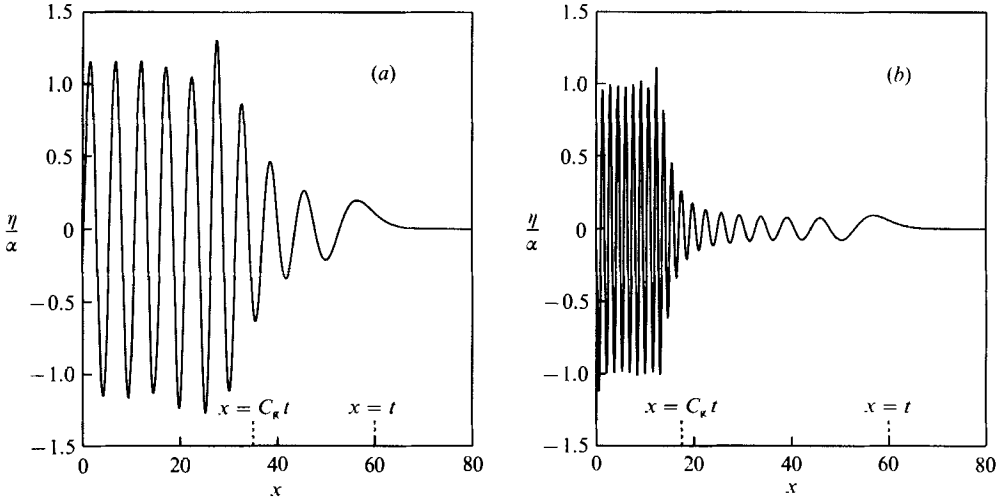
FIGURE 7. Free-surface elevations for the simple-harmonic velocity at $t = 60$ when surface tension $T = 0$: (a) $\omega = 1$; (b) $\omega = 2$.

6.2. *Harmonic analysis of a general wavemaker velocity*

As a final example, the velocity of a wavemaker given by a Fourier cosine series

$$u(t) = \sum_{n=1}^{N} a_n \cos(\omega_n t - \theta_n) \tag{73}$$

is considered. A straightforward application of (27) gives

$$A = \frac{2}{\pi} \frac{\beta}{k^2 \cosh k} \sum_{n=1}^{N} \frac{a_n}{\omega_n^2 - \beta^2} [\omega_n \sin \theta_n \sin \beta t - \beta \cos \theta_n \cos \beta t + \beta \cos(\omega_n t - \theta_n)]. \tag{74}$$

We then follow the same procedure as before to obtain

$$\eta = \frac{2\alpha}{\pi} \int_0^\infty \left[\sum_{n=1}^{N} a_n \frac{\omega_n \sin(\omega_n t - \theta_n) + \omega_n \sin \theta_n \cos \beta t - \beta \cos \theta_n \sin \beta t}{\omega_n^2 - \beta^2} \right] \tanh k \cos kx \frac{dk}{k} + O(\alpha^2). \tag{75}$$

We take $N = 72$ and $T = 0$ and use the Fourier cosine coefficients of the wavemaker velocity provided by Dommermuth *et al.* (1988). Figure 8 compares the free-surface elevations against time at three different locations to the wave-probe measurements of Dommermuth *et al.* (1988). We have chosen to include only the extrema of their figures for clarity. They also show a linear result based on Fourier series representation for a tank of finite length, which agrees well with the present result away from the wavemaker. For a moderate distance from the wavemaker ($x = 3.17$), the free-surface elevation (75) shows good agreement with the experimental measurements. Farther away from the wavemaker ($x = 9.17$), the nonlinear effects have accumulated, and the agreement becomes less satisfactory. As shown in the previous sections, surface tension affects the free-surface configuration primarily very near the wavemaker ($x \ll t^2$) and for small time, so it is neglected in these comparisons.
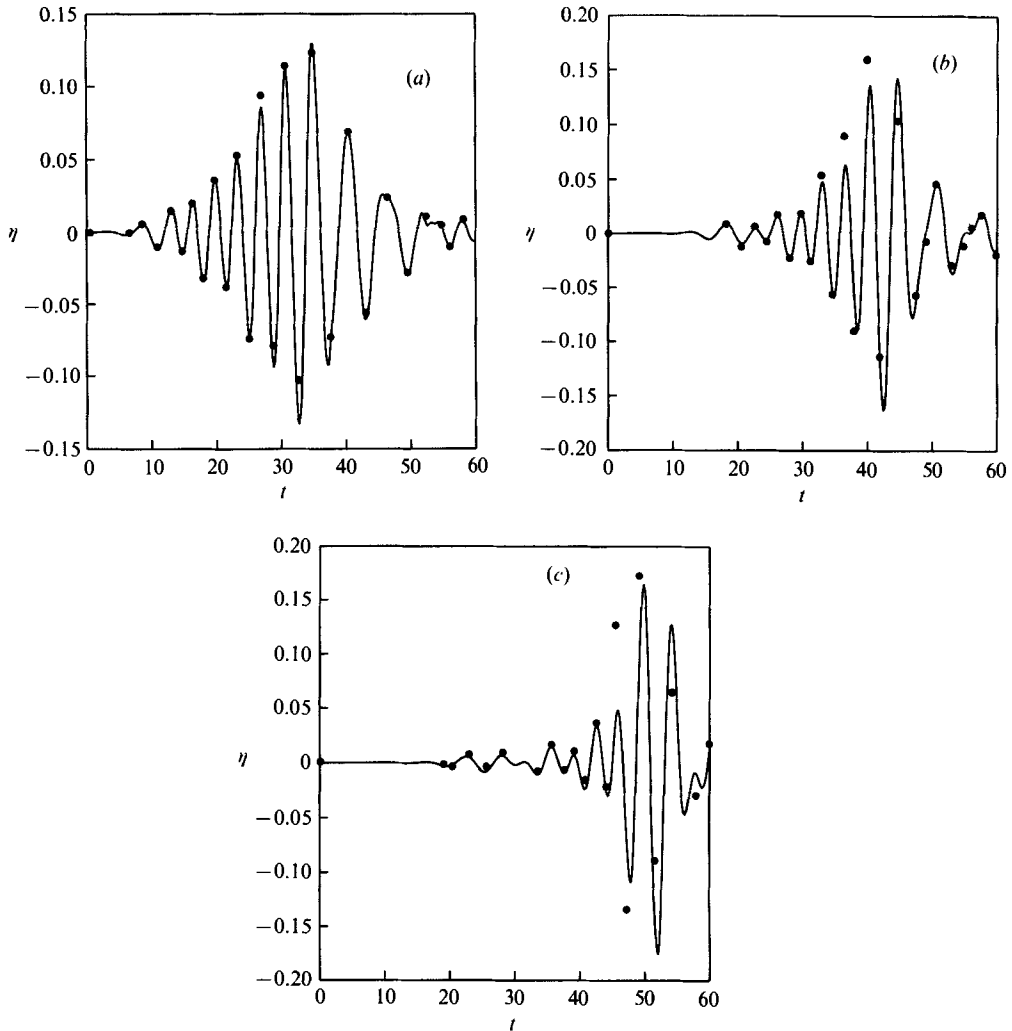
FIGURE 8. Free-surface elevations according to present method (——) and compared to experimental measurements (●) of Dommermuth *et al.* (1988): (*a*) $x = 3.17$; (*b*) $x = 5$; (*c*) $x = 10$.

7. Concluding remarks

To avoid an artificial singularity at the contact line between the free surface and the wavemaker introduced by the small-time expansion, a Fourier-integral method is developed for small Froude number. This method yields solutions for general wavemaker velocities that need not be given as powers of time. It also allows, with little added effort, the study of the capillary effects.

In the absence of surface tension, an infinite number of small-scale wiggles is present near the wavemaker, as shown also in the local solution of Roberts (1987) for small time, and the contact angle has a jump at $t = 0$. Surface tension suppresses the wiggles and maintains the contact angle at its initial static value. Far from the wavemaker, effects of surface tension become less important. For consistent and realistic results, surface tension should be considered near the contact line.

When the acceleration of the wavemaker is sufficiently large, the present linear solution is not valid near the wavemaker for very small time. A correct inner solution

for these conditions requires a fully nonlinear formulation. Even when the acceleration is small, the solution is not analytic because the wavemaker velocity is not analytic at $t = 0$. Successive differentiation in space or time will eventually make the expansion non-uniformly valid near the origin.

The large-time behaviour for the wavemaker moving with constant velocity is also obtained. The contact-line elevation approaches a value equal to the Fronde number, and the free surface behind the wave front can be approximated by a wavetrain superimposed on a flat surface. Beyond the wave front, which moves with the phase velocity for shallow water, the free-surface elevation decreases exponentially to the undisturbed value, zero. For the simple-harmonic wavemaker, the large-time behaviour agrees with the steady-state solution of Havelock (1929) behind the wave front but far from the wavemaker.

A general wavemaker velocity given by a Fourier cosine series is considered, and the free-surface elevation is compared with the experimental results of Dommermuth *et al.* (1988). The agreement with the wave-probe measurements is excellent at moderate distances from the wavemaker for all time and becomes less satisfactory farther away from the wavemaker for large time, when the nonlinear effects have accumulated.

REFERENCES

ABRAMOWITZ, M. & STEGUN, I. A. 1965 *Handbook of Mathematical Functions*, pp. 447–449. Dover.

CHWANG, A. T. 1983 Nonlinear hydrodynamic pressure on an accelerating plate. *Phys. Fluids* **25**, 383–387.

DOMMERMUTH, D. G., YUE, D. K. P., CHAN, E. S. & MELVILLE, W. K. 1988 Deep water plunging breakers: a comparison between potential theory and experiments. *J. Fluid Mech.* **189**, 423–442.

DUSSAN V., E. B. 1979 On the spreading of liquids on solid surfaces: static and dynamic contact lines. *Ann. Rev. Fluid Mech.* **11**, 371–400.

GRADSHTEYN, I. S. & RYZHIK, I. M. 1980 *Table of Integrals, Series, and Products*, p. 516. Academic.

HAVELOCK, T. H. 1929 Forced surface-waves on water. *Phil. Mag.* **8**, 569–576.

HOCKING, L. M. 1987 The damping of capillary–gravity waves at a rigid boundary. *J. Fluid Mech.* **179**, 253–266.

JOO, S. W., MESSITER, A. F. & SCHULTZ, W, W. 1988 Evolution of nonlinear waves due to a moving wall. *3rd Intl Workshop on Water Waves and Floating Bodies, Woods Hole, MA.*

KENNARD, E. H. 1949 Generation of surface waves by a moving partition. *Q. Appl. Maths.* **7**, 303–312.

LIN, W. M. 1984 Nonlinear motion of the free surface near a moving body. Ph.D. thesis, MIT, Dept. of Ocean Engineering.

MADSEN, O. S. 1970 Waves generated by a piston-type wavemaker. *12th Coastal Engng. Conf. Proc.*, pp. 589–607. ASCE.

PEREGRINE, D. H. 1972 Flow due to a vertical plate moving in a channel. Unpublished note.

ROBERTS, A. J. 1987 Transient free-surface flows generated by a moving vertical plate. *Q. J. Mech. Appl. Maths* **40**, 129–158.

SCHULTZ, W. W. & HONG, S. W. 1989 Solution of potential problems using an overdetermined complex boundary integral method. *J. Comput. Phys.* **84**, 414–440.

YIH, C. S. 1979 *Fluid Mechanics*, pp. 195–197. West River Press.